Volume 1 | Number 1 | Jan 2013 | Pages 1–100

Journal of
Materials Chemistry A

Materials for energy and sustainability
www.rsc.org/materialsA

ROYAL SOCIETY
OF CHEMISTRY

ROYAL SOCIETY
OF CHEMISTRY

www.rsc.org/materialsA

Remarkable stability of unmodified GaAs photocathodes during hydrogen evolution in acidic electrolyte

J. L. Young,[a,b] K. X. Steirer,[a] M. J. Dzara,[c] J. A. Turner,[a] and T. G. Deutsch[a]

[a]National Renewable Energy Laboratory, Golden, CO, 80401, USA
[b]Materials Science and Engineering Program, University of Colorado, Boulder, CO, 80309, USA
[c]Department of Chemical Engineering, Rochester Institute of Technology, Rochester, NY 14623, USA

We report on the remarkable stability of unmodified, epitaxially grown GaAs photocathodes during hydrogen evolution at -15 mA/cm^2 in 3M sulfuric acid electrolyte. Contrary to the perception regarding instability of III-V photoelecetrodes, results here show virtually no performance degradation and minimal etching after 120 hours.

Introduction

Established targets for solar-to-hydrogen (STH) efficiency, operating lifetime (stability), and absorber cost must be met before progress can be made toward large-scale, commercially viable photoelectrochemical (PEC) devices and systems that generate hydrogen (H$_2$) fuel from sunlight and water [1]. PEC electrodes and devices based on III-Vs have demonstrated high performance enabled by exceptional solid-state properties: direct bandgaps in the visible range, high absorption coefficients, long carrier lifetimes, and high mobilities. Khaselev and Turner also identified the stability challenges of semiconductors in PEC configurations that operate in contact with strongly acidic or basic electrolytes [2], as necessary to minimize solution conductivity losses and pH gradient overpotential [3]. GaAs is frequently used as the substrate in III-V epitaxy and as one of the absorbers in multi-junction photovoltaic (PV) devices. Its use as a substrate and bottom absorber in a monolithic, hybrid PV/PEC tandem with a lattice-matched top GaInP$_2$ PEC junction achieved a record 12.4% STH efficiency, but with limited stability [2]. A number of reports on the PEC stability of III-Vs exist [4][5][6][7], including those specific to p-GaAs in acid [8][9], which has led to a perception that GaAs and other high-performance photoelectrodes are generally unstable [10][11]. We held a similar perception [12] until recently re-evaluating the stability of unmodified, epitaxial p-GaAs used as control samples for our work on protective surface modification of III-V photocathodes [13]. Using a portfolio of photoelectrode durability characterization techniques, we present a clear example showing that p-GaAs photocathodes can have remarkable stability.

Experimental

We performed PEC durability testing and characterized the photocathodes using microscopy, profilometry, elemental analysis of testing electrolytes, and X-ray photoelectron spectroscopy (XPS) measurements to evaluate the stability of p-GaAs. Two μm-thick epitaxial GaAs Zn-doped p-type to 10^{17} cm^{-3} were grown by organometallic vapor-phase epitaxy on 3"-diameter degenerately p-doped GaAs(100) substrate wafers 4° offcut toward 111B. Ohmic contacts were made to the back by evaporating Ti/Au. The wafer was then cleaved into ~8x8-mm squares to be used as photocathodes. PEC characterization and durability testing were performed in a custom compression cell (Figure S1) in which a thin washer punched from Kalrez® (DuPont™) sheet stock was used to create a seal to the samples and define a 0.185-cm^2 photoelectrode surface area. A spring-loaded Au-plated stainless-steel plunger compressed the p-GaAs sample and washer onto an opening in the glass PEC cell body to create a seal, while also serving as an electrical lead to the back contact. We performed the durability tests using a compression cell because the easy disassembly facilitates post-durability analysis. The cell body was filled with 3M H$_2$SO$_4$ with 1 mM Triton X-100 (both OmniTrace® EMD Millipore) surfactant added to expedite H$_2$ bubble evolution. Because surfactant improves stability [14], we compare p-GaAs to p-GaInP$_2$ here and to p-InP from past work [13]; all tested in the same electrolyte solution with added surfactant. A 1-cm x 2.5-cm Pt foil counter electrode (anode) was contained in a glass tube with a medium-porosity glass frit end that was inserted into a port on the PEC cell body. The glass tube was

filled with the same 3M H_2SO_4 but without surfactant, a practice we found to mitigate counter electrode fouling and solution yellowing previously observed by our group [13], presumably due to surfactant degradation at the anode. We used a $Hg/HgSO_4$ reference electrode (MSE) from Koslow Scientific Co. having a reference potential of 0.634 V vs. normal hydrogen electrode (NHE). Its filling solution being the same as the electrolyte (3M H_2SO_4) eliminates concentration gradients that would cause the reference potential to drift over long-term testing. We note that stability testing was also performed in a variety of configurations: epoxy-mounted electrodes [12] instead of a compression cell, without a glass frit separating the photocathode from the counter electrode, and with Zonyl FSN-100 fluorosurfactant instead of Triton X-100—all with excellent results—showing that stability is independent of these testing conditions. The illumination source was a 250-W quartz tungsten halogen lamp with water filter and light-shaping diffuser (Newport) with intensity set to match the current from a Si reference cell calibrated to an AM1.5G spectrum. The p-GaAs durability testing was performed at a constant -15 mA/cm^2 current while continuously monitoring the working electrode's potential vs. MSE. Chopped-light current-voltage (CLIV) measurements were taken before and after each durability test with the voltage scanned at 20 mV/s while blocking/unblocking the light source at 0.1-V intervals. The electrolyte analyzed for dissolved Ga and As by inductively coupled plasma mass spectrometry (ICP-MS) and the quantity detected (in ppb) was converted to nanomoles. The surface profiles were measured with both optical (Veeco) and stylus (Dektak 8 with 5-µm tip) profilometry and the surface morphology was examined with a JEOL JSM-7000F scanning electron microscope (SEM) equipped with energy-dispersive X-ray spectroscopy (EDS).

Results

We performed baseline chemical stability testing of p-GaAs in the dark at open circuit for 96 hours. Stereomicroscopy showed a pristine surface and profilometry showed negligible etching (Figure S2). The lack of etching is unexpectedly different than the statement by Walczak et al. that high-performance photolectrodes such as GaAs would dissolve quickly in electrolyte solution near pH 0 [11]. This intrinsic chemical stability is important to survive the diurnal cycle of solar radiation and demonstrates that the corrosion resistance is not exclusively due to cathodic protection [15] [16]. Figure 1a shows CLIVs performed before durability testing that have a light-limited photocurrent (LLPC) of -22 mA/cm^2 and photocurrent onset potential of -0.7 V vs. MSE. After durability tests lasting 72 and 120 h, the p-GaAs shows a slight cathodic shift in photocurrent onset potential, but also a slight increase in fill factor due to the steeper rise in photocurrent. This compares to a p-GaInP$_2$ photocathode before (0 h) and after just a 1 h durability test at -10 mA/cm^2, which showed a large cathodic shift in photocurrent onset potential (-400 mV) and a 2–3 mA/cm^2 decrease in LLPC. The small increase in p-GaAs current density at 72 and 120 h is, in part, due to a small amount of dark current (1–2 mA/cm^2), but also due to increased light absorption discussed later. After letting the sample tested for 120 h sit in the dark in electrolyte at open circuit for 0.5 h, the dark current was reduced and the LLPC closely matched the CLIV taken before durability testing (0 h). Figure 1b shows the potential of the p-GaAs photocathodes monitored vs. MSE throughout galvanostatic durability testing at -15 mA/cm^2. The p-GaAs starts out at -0.9 V vs. MSE, matching the operation point of the CLIV in Figure 1a, and then became 50–100 mV more positive during the first 1–2 hours before increasing in magnitude and stabilizing around -1 V vs. MSE over the next 10 hours. The 24 h and 96 h runs were stopped and restarted at 18 h and 72 h, respectively, as indicated by the '#' marker. Upon restarting after less than one minute rest time, the operating potentials recovered to their initial -0.9 V vs. MSE operating point and again improved ~50 mV over the next hour before slowly increasing in magnitude over the next few hours.

The sample tested for 120 hours was photographed with a stereomicroscope, characterized with optical and stylus profilometry, and examined with SEM (Figure 2). Figure 2a shows a stereoscope image of the p-GaAs with the active photocathode area encircled by a black dotted line. The perimeter that was under or outside of the washer during testing is specular; whereas the majority of the active region has a darker, slightly brown appearance except at the top, where a lip created by the washer would accumulate some H_2 bubbles. Optical profilometry (Figure 2b) was taken with the reference height established by the unexposed perimeter (green), and it showed minimal etching throughout the lower

two-thirds of the active region and some etching in the upper right, perhaps due to higher current densities associated with its proximity to the counter electrode. Etch profiles were confirmed with stylus profilometry (Figure 2c) scanned from the perimeter into the active region at the locations indicated by letters A–G in Figure 2b. The etch depths ranged from 5–45 nm and revealed a texture with amplitude 5–15 nm in the active region. This etch rate (<0.5 nm/h) for p-GaAs is remarkably low compared to the etch rate of unmodified p-GaInP$_2$ at -10 mA/cm^2 (40–80 nm/h) and unmodified p-InP at -25 mA/cm^2 (170 nm/h) where 1–2 μm for p-GaInP$_2$ [17] and 4 μm of p-InP [13] were removed within 24 h. An etch rate two orders of magnitude lower than other unmodified III-Vs is significant. The darker appearance of the p-GaAs region exposed to electrolyte (Figure 2a) and texturing (Figure 2c) suggest the presence of antireflective properties, which corroborates with the higher LLPC measured after durability testing (Figure 1a). The larger texture in the region that was underneath the washer was determined by EDS to be carbon particles, likely residue of carbon black which is a filler used in perfluoroelastomers such as Kalrez®. The texturing within the active region appears to correspond with a dispersion of particles (bright dots) observed with SEM (Figure 2d). Although not surface sensitive, EDS indicated that the active region is ~2 at. % points more As-rich compared to the 50:50 at. % GaAs stoichiometry of the area outside of the washer.

To evaluate the surface composition, XPS was used to characterize p-GaAs surfaces after 1, 24, and 96 h (Figure 1b) of durability testing. After PEC testing, samples were extracted from the PEC cell in an Ar-filled glove box to eliminate exposure to air. XPS was performed using a Physical Electronics 5600 photoelectron spectrometer with monochromatic Al Kα excitation (pressure < 2×10^{-10} torr). Multipoint binding-energy calibration followed M.P. Seah for Au 4f$_{7/2}$, Ag 3d$_{5/2}$ and Cu 2p$_{3/2}$ peak centriods [18]. Pass energy was 11.75 eV. Compositions were calculated using Multipak software values. Two baseline samples were included for comparison. The first sampled, labeled "solvent wash" in Figure 3, was rinsed with acetone, methanol, and then submerged in Ar-sparged deionized (DI) water before transferring to ultra-high vacuum (UHV). The second sample was similarly cleaned and then soaked for 1 h in the PEC electrolyte before rinsing and transferring to UHV. XPS spectra for As 2p$_{3/2}$ (Figure 3), Ga 2p$_{3/2}$, and O 1s (Figure S4) regions were analysed to develop an understanding of the changes induced under PEC conditions. Figure 3 shows the As 2p$_{3/2}$ spectral region deconvoluted with Gauss-Lorentz (80/20) and Shirley background model fits. Residuals are also shown. The high binding-energy (BE) core level regions were chosen for enhanced surface sensitivity because the photoelectrons detected from the Ga 2p$_{3/2}$ and As 2p$_{3/2}$ are emitted from the top 0.8–1.2 nm [19]. A summary of the modeled composition is reported in Table S1. Peak positions were restricted to within ±0.1 eV while simultaneously fitting all the spectra. Following literature, the As 2p$_{3/2}$ spectra (Figure 3) were fit with five peaks including lattice As (1322.7 eV), As^0 (1323.7 eV), As$_2$O$_3$ (1325.8 eV), and a mixed oxide (1327.2 eV) whereas the As 2p$_{3/2}$ peak (1321.3 eV) was tentatively assigned to As dimers (1321.3 eV) following similar As 3d spectral features. Mixed oxides observed for Ga 2p$_{3/2}$ peak (1118.7 eV) and As 2p$_{3/2}$ peak (1327.2 eV) spectra are native oxides formed while exposed to air [20].

Discussion

The evolution of the observed surface species and their electrochemical stability under the p-GaAs photocathode operating conditions can provide insight into the stabilization mechanism. Pourbaix provides pH-potential diagrams for Ga and As in contact with electrolyte [21]. For a pH = -0.5 (3M sulfuric acid), the thermodynamically preferred state of Ga is aqueous Ga^{3+} ions for potentials more positive than ca. -0.6 V vs. NHE (all subsequent potentials are vs. NHE unless otherwise stated), whereas atomic Ga is favored at more negative potentials. For As, the stable and insoluble species at pH =-0.5 are As$_2$O$_3$ for potentials 0.2 to 0.6 V and As for -0.5 to 0.2 V. From our observation of negligible etching after 96 h at open-circuit potential (OCP), we can conclude that the surface potential at OCP is within one of these stable ranges. Furthermore, the surface potential at OCP must be within the water-splitting half-reaction potentials (0–1.23 V), which means that the stable Ga and As species are dissolved Ga^{3+} and either As$_2$O$_3$ or As. In agreement, we observed that the native mixed oxide (potentially including GaAsO$_4$, Ga$_2$O$_5$, As$_2$O$_5$, and others) is removed by soaking in electrolyte for just one hour, leaving As and As$_2$O$_3$ as the likely candidates for p-GaAs etch resistance at OCP (Figure 3a,b).

During H_2 evolution, the surface potential is more negative than the hydrogen evolution reaction (HER) potential, but the potential at which electrons reach the electrolyte or conduction-band position is not known precisely due to the possibility of Fermi-level pinning/unpinning [22][23] or band-edge migration [24]. The operating pH is -0.5, but now may be slightly more positive in the near-surface region as protons are consumed at -15 mA/cm^2. However, the high 3M bulk acid concentration and vigorous stirring of copious H_2 bubbling at the surface limit significant deviation [25]. If we assume a kinetic overpotential for H_2 evolution of less than 0.5 V on p-GaAs, the surface potential is within -0.5 V of the HER. Here, Pourbaix diagrams suggest that As, but not As_2O_3, is stable under H_2 evolution, which agrees with the relative increase of As over As_2O_3 in the samples that were durability tested for 1 h (Figure 3c) and 24 h (Figure 3d) compared to the sample soaked in electrolyte at OCP for 1 h (Figure 3b). At OCP, Ga will dissolve as Ga^{3+}, leaving As the more likely surface-stabilizing species. We note that if the surface potential is more negative than -0.5 V, Ga and AsH_3 are the preferred species. Practically, such a large operating potential above HER is unsuitable because of the voltage loss of the excess overpotential. Photocathodes modified with attached Pt catalysts may have < 100 mV overpotential [26][27]; but full discussion of the intrinsic stability of unmodified p-GaAs includes consideration of high overpotential. Here, Pourbaix suggests that Ga rather than As could passivate the surface, and previously dissolved Ga^{3+} in solution could be reduced to Ga on the photoelectrode surface. Park and Barber's thermodynamic analysis of GaAs gives a narrow potential range for the stability of As, making this a more likely explanation for GaAs stability according to their analysis. However, As and As_2O_3 on GaAs is a common experimental observation after etching in acid [28][29][30]. Our quantification of Ga and As in solution (Figure 2e) shows 2:1 and 1:2 Ga:As ratios for the shortest and longest durability testing times, respectively. This supports a model where excess As stabilizes the surface initially and some Ga^{3+} in solution is redeposited after 120 hours. However, a systematic trend connecting these endpoints though the intermediate durability testing times is not yet clear. A change in surface stoichiometry would imply that selective corrosion contributes to photocurrent if occurring as electrochemical reduction. We calculate that a 50 nm etch depth amounts to 2.2×10^{17} atoms removed (GaAs atomic density 4.4×10^{22} cm^{-3} [31]) that contribute 3 electrons each to supply a total of 0.020 C toward corrosion reactions. During the 120 hr durability test at -15 mA/cm^2, a total of 1,200 C pass through the 0.185-cm^2 photoelectrode. Therefore, the fraction of corrosion current is negligible at 17 parts per *million* of the photocurrent.

The stable species at OCP are relevant because the p-GaAs photoelectrode returns to OCP upon stopping the durability test. The electrode potential reverts to its original potential upon simply pausing and restarting the durability test (indicated by '#' in Figure 1b). We previously noted that As_2O_3 should not form during hydrogen evolution but that As can convert to As_2O_3 after stopping the durability test, both of which we detect with XPS. This is supported by a brown appearance of the surface (Figure 1a) that Smeenk et al. also characterized as predominantly elemental As with a small signal from As_2O_3. We also consistently detected Ga_2O_3 in all samples, which, in contrast to As and As_2O_3, the Pourbaix diagram for Ga shows that Ga_2O_3 is only stable at more neutral pH values. The Ga_2O_3 we observe may have formed from As_2O_3 reacting with GaAs to form Ga_2O_3 and elemental As, which are stable phases in contact with GaAs [29]. If the Ga_2O_3 formed during operation, it is plausible that it is also protected, like GaAs, by the As overlayer. Alternatively, the gallium oxide may have also formed during the pH shift of the DI water rinse, as observed by Vilar et al. [29]. The likelihood of oxidation at OCP combined with surface roughness for long durability testing time (Figure 2a–d) explain the increased amount of As_2O_3 (Figure 3e) and Ga_2O_3 (Figure S4e) relative to As and Ga, respectively, detected after 96 hours.

The surface-stabilizing candidates of As_2O_3 and As were identified for p-GaAs in pH = -0.5 at OCP. Under H_2 evolution, As is a more likely candidate, but we noted that Ga rather than As is stable at surface potentials more negative than ca. -0.5 V. We discussed the likelihood that species detected that are not expected to be stable during operation (Ga_2O_3 and As_2O_3) formed after stopping the durability testing.

The observed stability of GaAs is remarkable and in strong contrast to $GaInP_2$ and InP. Although the Pourbaix diagrams for Ga and In are similar, As contrasts with that of P where P is expected to form

soluble phosphates or phosphites. When excess As is left at the GaAs|electrolyte interface, the photoelectrochemical junction may be better represented by a GaAs|As Schottky model. Here, the junction-forming layers responsible for photovoltage reside in the solid state. The GaAs|As|electrolyte multilayer structure affords stable performance while the As overlayer is thin enough to be highly transparent, thus maintaining high photocurrents. We note it is important that As has a low work function (3.75 eV [32]) necessary to maintain a Schottky junction to p-GaAs, rather than a high work function that could cause an Ohmic contact and loss of photovoltage. We note that an electrochemical stability regime similar to that of As also exists for Sb and Bi in column V below As, but not for P and N above. III-V arsenide and the less studied III-V antimonide and bismide photocathodes warrant further investigation.

Although not explored here, impurities and crystal defects can enhance etch rates [33]–[36]; thus, variation in material quality could be responsible for the discrepancy among reports on the stability of GaAs. In going beyond the GaInP$_2$/GaAs tandems that have demonstrated 12.4% STH, lower bottom and top absorber bandgaps are necessary [37], which will lead into exploration of other III-V ternary and quaternary alloys that incorporate GaAs (e.g., GaInAsP, InGaAs) and could also be stable. We do not expect intrinsic stability to alleviate the need for stabilizing photoelectrode surfaces with catalysts and/or coatings. However, high-performance photoelectrodes that exhibit *intrinsic stability* should be more robust templates for achieving the multi-year operational lifetimes necessary for commercially viable PEC devices.

Conclusions

We characterized unmodified, p-GaAs photocathodes during hydrogen evolution in acidic electrolyte and found them to be remarkably stable—having two orders of magnitude slower etch rate than unmodified p-GaInP$_2$ and p-InP. This new finding among PEC corrosion studies is contrary to earlier reports and popular perception in the field toward universal instability of III-V high-performance photocathodes. We discussed a set of candidate species detected with XPS after durability testing that could contribute to stabilizing the p-GaAs/electrolyte interface. Analysis supports that this remarkable corrosion resistance likely results from the formation of elemental As during PEC conditions.

Acknowledgements

References

[1]   "Department of Energy Fuel Cell Technologies Office Multi-year Research, Development, and Demonstration Plan," 2015. [Online]. Available: http://energy.gov/sites/prod/files/2015/06/f23/fcto_myrdd_production.pdf.

[2]   O. Khaselev and J. A. Turner, "A Monolithic Photovoltaic-Photoelectrochemical Device for Hydrogen Production via Water Splitting," *Science (80-.).*, vol. 280, no. 5362, pp. 425–427, 1998.

[3]   J. Jin, K. Walczak, M. R. Singh, C. Karp, N. Lewis, and C. Xiang, "An Experimental and Modeling/Simulation- Based Evaluation of the Efficiency and Operational Performance Characteristics of an Integrated, Membrane-Free, Neutral pH Solar-Driven Water-Splitting System," *Energy Environ. Sci.*, vol. 00, pp. 1–10, 2014.

[4]   O. Khaselev and J. A. Turner, "Electrochemical Stability of p-GaInP2 in Aqueous Electrolytes Toward Photoelectrochemical Water Splitting," *J. Electrochem. Soc.*, vol. 145, no. 10, p. 3335, 1998.

[5]   T. Bak, J. Nowotny, M. Rekas, and C. . Sorrell, "Photo-electrochemical hydrogen generation from water using solar energy. Materials-related aspects," *Int. J. Hydrogen Energy*, vol. 27, no. 10, pp. 991–1022, 2002.

[6]   J. O. Bockris and K. Uosaki, "The Rate of the Photoelectrochemical Generation of Hydrogen at p-Type Semiconductors," *J. Electrochem. Soc.*, vol. 124, no. 9, p. 1348, 1977.

[7]   P. Carlsson, B. Holmström, and L. Samuelson, "Stability towards photoelectrochemical etching in Ga (As,P) alloys," *J. Appl. Phys.*, vol. 63, no. 15, pp. 530–532, 1988.

[8]   S.-M. Park and M. E. Barber, "Thermodynamic stabilities of semiconductor electrodes," *J. Electroanal. Chem. Interfacial Electrochem.*, vol. 99, no. 1, pp. 67–75, 1979.

[9]   G. S. Weng, J. L. Luo, and D. G. Ivey, "Galvanic corrosion behavior of GaAs in acid solutions," *J. Vac. Sci. Technol. A Vacuum, Surfaces, Film.*, vol. 20, no. 3, p. 1015, 2002.

[10]   E. Verlage, S. Hu, R. Liu, R. J. R. Jones, K. Sun, C. Xiang, N. S. Lewis, H. A. Atwater, Jr., and H. A. Atwater, "A Monolithically Integrated, Intrinsically Safe, 10% Efficient, Solar-Driven Water-Splitting System Based on Active, Stable Earth-Abundant Electrocatalysts in Conjunction with Tandem III-V Light Absorbers Protected by Amorphous TiO2 Films," *Energy Environ. Sci.*, pp. 1–13, 2015.

[11]   K. Walczak, Y. Chen, C. Karp, J. W. Beeman, M. Shaner, J. Spurgeon, I. D. Sharp, X. Amashukeli, W. West, J. Jin, N. S. Lewis, and C. Xiang, "Modeling, Simulation, and Fabrication of a Fully Integrated, Acid-stable, Scalable Solar-Driven Water-Splitting System," *ChemSusChem*, vol. 8, pp. 544–551, 2015.

[12]   T. G. Deutsch, J. L. Head, and J. A. Turner, "Photoelectrochemical Characterization and Durability Analysis of GaInPN Epilayers," *J. Electrochem. Soc.*, vol. 155, no. 9, pp. B903–B907, 2008.

[13]   T. G. Deutsch and J. A. Turner, "Semiconductor Materials for Photoelectrolysis: 2014 U.S. DOE Hydrogen & Fuel Cells Program Review," 2014.

[14]   T. G. Deutsch, C. a. Koval, and J. a. Turner, "III-V nitride epilayers for photoelectrochemical water splitting: GaPN and GaAsPN," *J. Phys. Chem. B*, vol. 110, no. 50, pp. 25297–25307, 2006.

[15]   A. Heller, "Hydrogen-evolving solar cells," *Science*, vol. 223, no. 4641, pp. 1141–8, 1984.

[16]   F. R. F. Fan and A. J. Bard, "Semiconductor electrodes. 24. Behavior of photoelectrochemical cells based on p-type gallium arsenide in aqueous solutions," *J. Am. Chem. Soc.*, vol. 102, no. 11, pp. 3677–3683, 1980.

[17]   J. Turner, T. Deutsch, H. Wang, A. Welch, and M. Al-jassim, "II.F.2 Semiconductor Materials for Photoelectrolysis," *DOE Hydrogen and Fuel Cells Program FY 2012 Annual Progress Report.*, 2012. [Online]. Available: http://www.hydrogen.energy.gov/pdfs/progress12/ii_f_2_turner_2012.pdf.

[18]   M. P. Seah, "Post-1989 Calibration Energies for X-ray Photoelectron Spectrometers and the 1990 Josephson Constant," *Surf. Interface Anal.*, vol. 14, no. 488, pp. 552–553, 1989.

[19]   W. Monch, "Electronic Characterization of Compound Semiconductor Surfaces and Interfaces," *Thin Solid Films*, vol. 104, pp. 285–299, 1983.

[20]   C. M. Demanet and M. A. Marais, "A multilayer model for GaAs oxides formed at room temperature in air as deduced from an XPS analysis," *Surf. Interface Anal.*, vol. 7, no. 1, pp. 13–16, 1985.

[21]   M. Pourbaix, *Atlas of Electrochemical Equilibria in Aqueous Solutions*, 2nd ed. National Association of Corrosion Engineers, 1974.

[22]   A. J. Bard, A. B. Bocarsly, F. F. Fan, E. G. Walton, and M. S. Wrighton, "The concept of fermi level pinning at semiconductor/liqud junctions. Consequences for energy conversion efficiency and selection of useful

redox couples in solar devices," *J. Am. Chem. Soc.*, vol. 102, no. 11, 1980.

[23]   S. D. Offsey, J. M. Woodall, a. C. Warren, P. D. Kirchner, T. I. Chappell, and G. D. Pettit, "Unpinned (100) GaAs surfaces in air using photochemistry," *Applied Physics Letters*, vol. 48, no. 7. pp. 475–477, 1986.

[24]   A. Bansal and J. Turner, "Suppression of band edge migration at the p-GaInP2/H2O interface under illumination via catalysis," *J. Phys. Chem. B*, vol. 104, pp. 6591–6598, 2000.

[25]   M. R. Singh, K. M. Papadantonakis, C. Xiang, and N. Lewis, "An Electrochemical Engineering Assessment of the Operational Conditions and Constraints for Solar-Driven Water-Splitting Systems at Near-Neutral pH," *Energy Environ. Sci.*, 2015.

[26]   M. F. Weber and M. J. Dignam, "Efficiency of Splitting Water with Semiconducting Photoelectrodes," *J. Electrochem. Soc.*, vol. 131, no. 6, p. 1258, 1984.

[27]   M. G. Walter, E. L. Warren, J. R. McKone, S. W. Boettcher, Q. Mi, E. a Santori, and N. S. Lewis, "Solar Water Splitting Cells," *Chem. Rev.*, vol. 110, pp. 6446–6473, 2010.

[28]   N. J. Smeenk, J. Engel, P. Mulder, G. J. Bauhuis, G. M. M. W. Bissels, J. J. Schermer, E. Vlieg, and J. J. Kelly, "Arsenic Formation on GaAs during Etching in HF Solutions: Relevance for the Epitaxial Lift-Off Process," *ECS J. Solid State Sci. Technol.*, vol. 2, no. 3, pp. P58–P65, 2012.

[29]   K.-H. Kretschmer and H. L. Hartnagel, "XPS-Analysis of GaAs-Surface Quality Affecting Interelectrode Material Migration," *23rd Int. Reliab. Phys. Symp.*, pp. 45–48, 1985.

[30]   M. Rei Vilar, J. El Beghdadi, F. Debontridder, R. Artzi, R. Naaman, a. M. Ferraria, and a. M. B. Do Rego, "Characterization of wet-etched GaAs (100) surfaces," *Surf. Interface Anal.*, vol. 37, no. 8, pp. 673–682, 2005.

[31]   M. Levinshtein, S. Rumyantsev, and M. Shur, "Volume 1 Si, Ge, C (Diamond), GaAs, GaP, GaSb, InAs, InP, InSb," in *Handbook Series on Semiconductor Parameters*, 1996.

[32]   J. G. Speight, *Lange's Handbook Of Chemistry, 16th ed.* 2005.

[33]   D. J. Stirland and B. W. Straughan, "A review of etching and defect characterisation of gallium arsenide substrate material," *Thin Solid Films*, vol. 31, no. 1–2, pp. 139–170, 1976.

[34]   A. Munoz-Yague and M. Bafleur, "Shallow defect etching of GaAs using AB solution under laser illumination," *J. Cryst. Growth*, vol. 53, no. 2, pp. 239–248, 1981.

[35]   A. R. Clawson, "Guide to references on III-V semiconductor chemical etching," *Mater. Sci. Eng.*, vol. 31, no. 1–6, pp. 1–438, 2001.

[36]   C. Frigeri, J. L. Weyher, S. Müller, and P. Hiesinger, "Analysis of peculiar structural defects created in GaAs by diffusion of copper," *J. Cryst. Growth*, vol. 210, no. 1, pp. 177–181, 2000.

[37]   H. Döscher, J. F. Geisz, T. G. Deutsch, and J. A. Turner, "Sunlight absorption in water – efficiency and design implications for photoelectrochemical devices," *Energy Environ. Sci.*, vol. 7, no. 9, pp. 2951–2956, 2014.
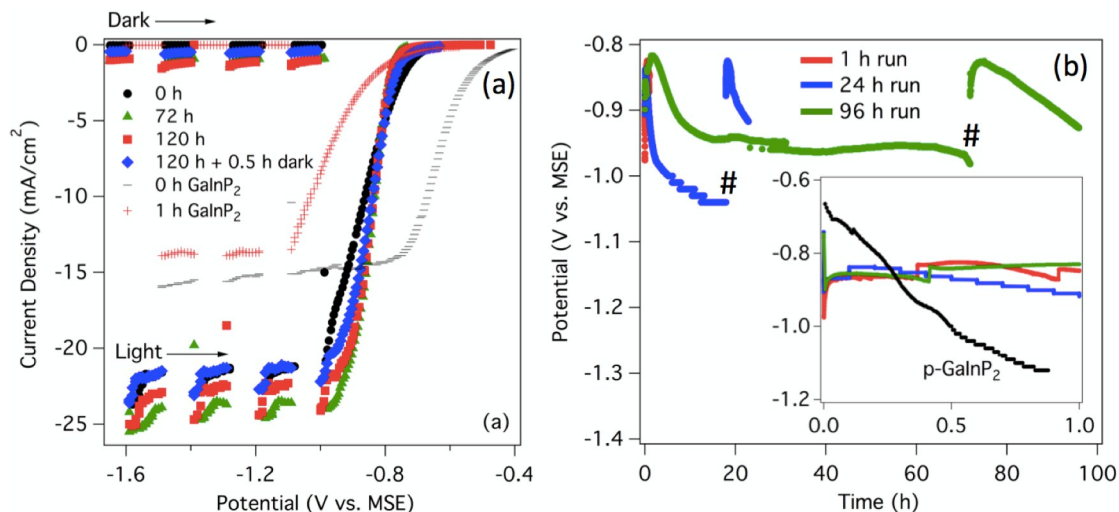
Fig. 1 (a) CLIV characterization of p-GaAs photocathodes before (0 hr, black dots), after 72 hr (green triangles), and 120 hr (red squares) galvanostatic durability testing at -15 mA/cm². The 120 hr sample was measured again after 0.5 hr at open circuit in the dark (blue diamonds). This is compared to a p-GaInP$_2$ photocathode before (0 hr) and after 1 hr durability testing. The "Light" and "Dark" labels indicate, respectively, the current measured under illumination and with the illumination blocked. (b) The p-GaAs potential monitored vs. MSE during durability testing for separate of samples tested for 1 hr (red), 24 hr (blue), and 96 hr (green). The durability tests paused at OCP and restarted are indicated at "#". The inset shows the first hour of testing compared to p-GaInP$_2$ (black).
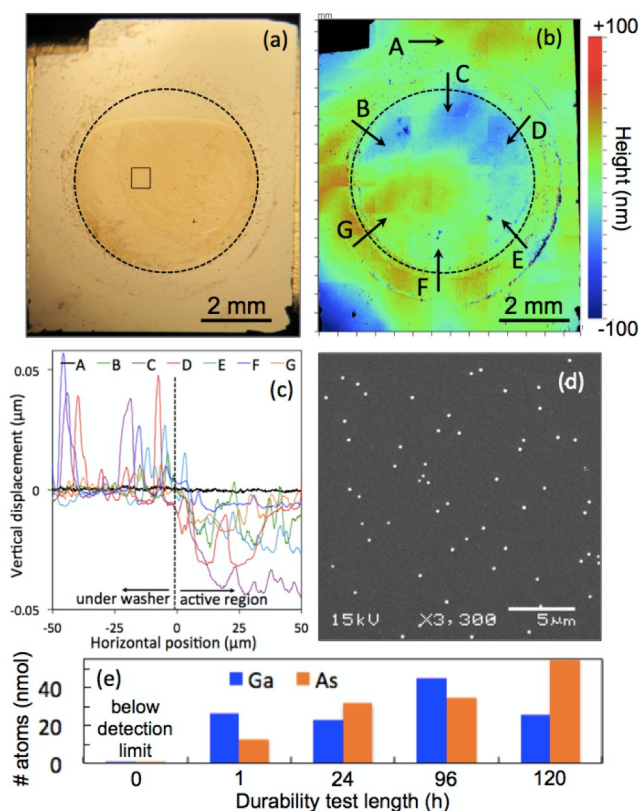

Fig. 2 (a) Stereoscope image after 120 hr testing with active region encircled by black dashed line. (b) Optical profilometry with height scale from -100 nm (dark blue) to +100 nm (dark red). (c) Stylus profilometry scans in the locations/directions indicated by letters A-G and arrows on (b). (d) SEM image of the active region at the location indicated with a black square in (a). (e) Quantification by ICP-MS in nanomoles (nmol) of Ga and As in the electrolyte after durability testing.
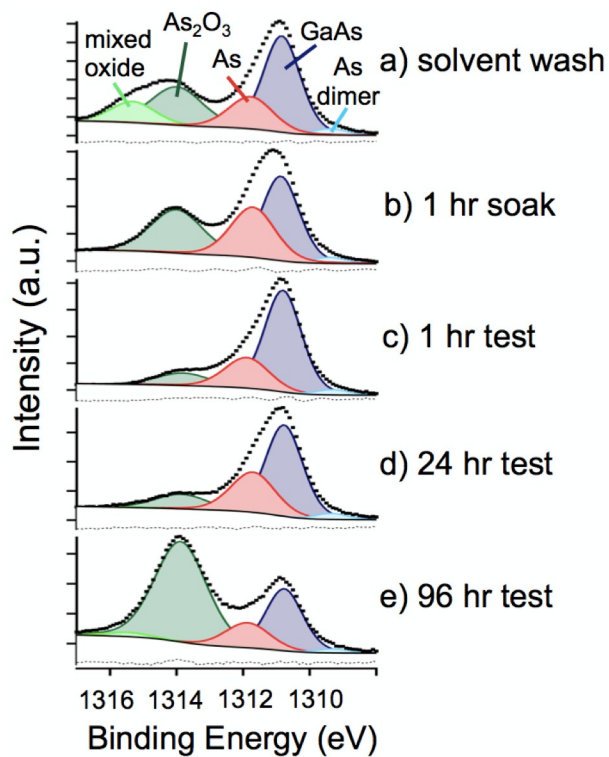
Fig. 3 XPS spectra of the As 2p3/2 core level is shown with the deconvoluted peak assignments. The two baseline samples were (a) solvent washed and (b) soaked in electrolyte for 1 hr. Three samples were durability tested for (c) 1 hr, (d) 24 hr, and (e) 96 hr before XPS measurements.